Electronic Supplementary Information

Chiral co-selector induced chirality switching in the enantioseparation of ofloxacin by forming co-crystal

Lichao He, Xinjian Chen, Xiangrong Li, Zhiyong Zhou and Zhongqi Ren**

College of Chemical Engineering, Beijing University of Chemical Technology, No. 15, North Third Ring Road East, Beijing 100029, People's Republic of China

Fax: 86 10 64197101; Tel: 86 10 64197101;

*E-mail:*renzq@mail.buct.edu.cn; zhouzy@mail.buct.edu.cn

Experimental Details

Sample Preparation.

Chemicals. RS-ofloxacin, S-ofloxacin, D-DBTA, L-DBTA, D-DMTA, L-DMTA, D-DTTA and L-DTTA were commercially available from Shanghai Aladdin biological technology co., LTD and were used as received without further purification. The water used in all experiments was prepared by filtration through an ultrapure purification system (Shanghai SKYLARK Industry Co., Ltd., Shanghai, China).

Separation Procedures. A novel liquid-solid two-phase system was selected to study the chiral selectivity transition process in the enantioseparation of racemic ofloxacin. The separation experiments were conducted in 100 mL conical flasks with cover. Equal volume (20mL) of ofloxaicn aqueous solution was added in the conical flask, followed by adding an appropriate amount of the combined resolving agents. The mixture was shaken sufficiently in a water bath at a fixed temperature and then left to equilibrate and settle for 50 min to ensure the formation of solid phase. At last, the mixture was separated by centrifugation and filtration. Then the concentrations of ofloxacin enantiomers in the aqueous phase were analyzed quantitatively with high performance liquid chromatography (HPLC).

Spectroscopy measurement

X-ray Powder Diffraction (PXRD). The PXRD investigations were carried out on a RigakuUltima IV X-ray Powder diffractometer (Tokyo, Japan) at 40 kV, 100 mA with a CuKα radiation (λ = 1.5406 Å). PXRD patterns were recorded from 5° to 40° in 2θ, with a scan rate of $1°\cdot min^{-1}$.

Fourier Transform Infrared Spectroscopy (FT-IR). FT-IR spectra have been recorded on a Nicolet 8700 attenuated total refection Fourier transform infrared spectrometer (Fisher Scientific, USA)in the range from 500 cm^{-1} to 4000 cm^{-1}.

Thermogravimetric Analysis (TGA). TGA measurements were performed ona TG thermal analyzer (TG209C, Netzsch, Germany) in a dynamic N_2 atmosphere. Approximate 10 mg samples were placed into aluminum pans and analyzed in the temperature rangingfrom 35 °C to 800 °C with a heating rate of $10\ °C\cdot min^{-1}$.

HPLC analysis method for ofloxacin. The chiral HPLC analysis was performed on a LC-20AT high performance liquid chromatograph (Shimadzu, Japan) equipped with anUV (SPD-20AT) detector and Zorbax Extend C18

column (length of 250 mm, internal diameter of 4.6 mm, particle size of 5μm) purchased from Agilent. The injection volume was 10 μL and column temperature was maintained at 39 °C. A mixed solution (50% ultrapure water, 50% methanol, v/v) with flow rate of 1 $mL \cdot min^{-1}$ was used for elution. The mobile phase consisted of methanol and aqueous solution (85:15, v/v) containing 10 $mmol \cdot L^{-1}$ L-leucine and 5 $mmol \cdot L^{-1}$ $CuSO_4$, which was employed at a flow rate of 0.8 $mL \cdot min^{-1}$. The effluent was monitored at 295 nm. The measured retention times for S-ofloxacin and R-ofloxacin were 15.5 min and 17.5 min, respectively.

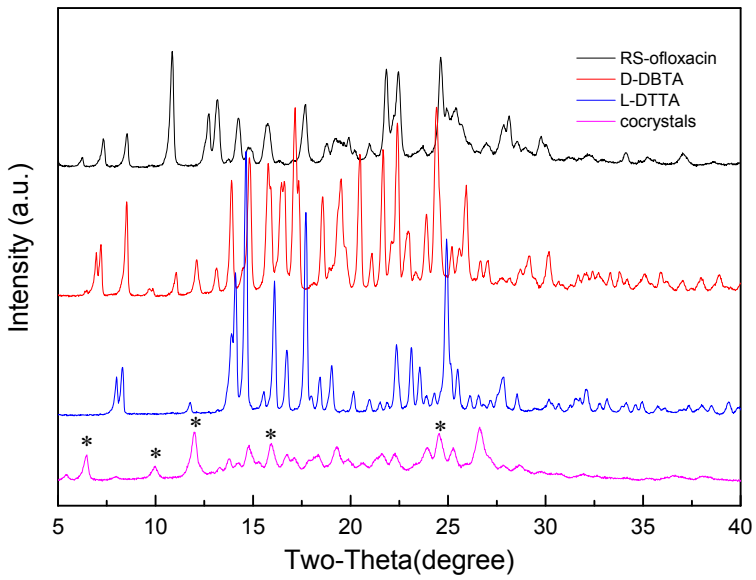

(a)

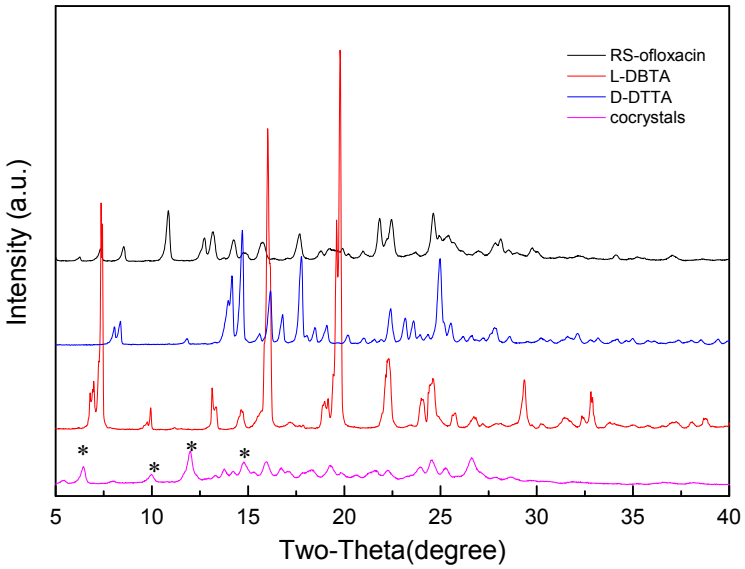

(b)

Figure. S1 PXRD curves of the co-crystals obtained after the chiral selectivity transition process (a, D-DBTA and L-DTTA as chiral selector; b, L-DBTA and D-DTTA as chiral selector)

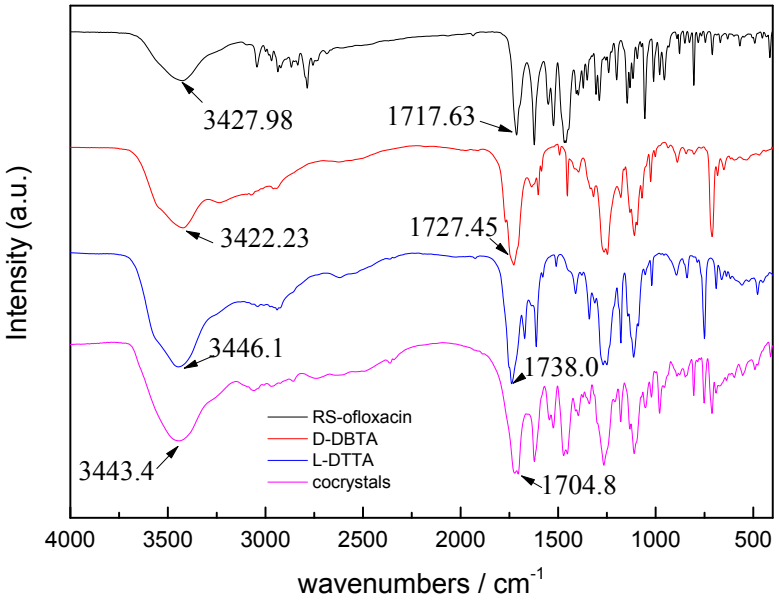

(a)

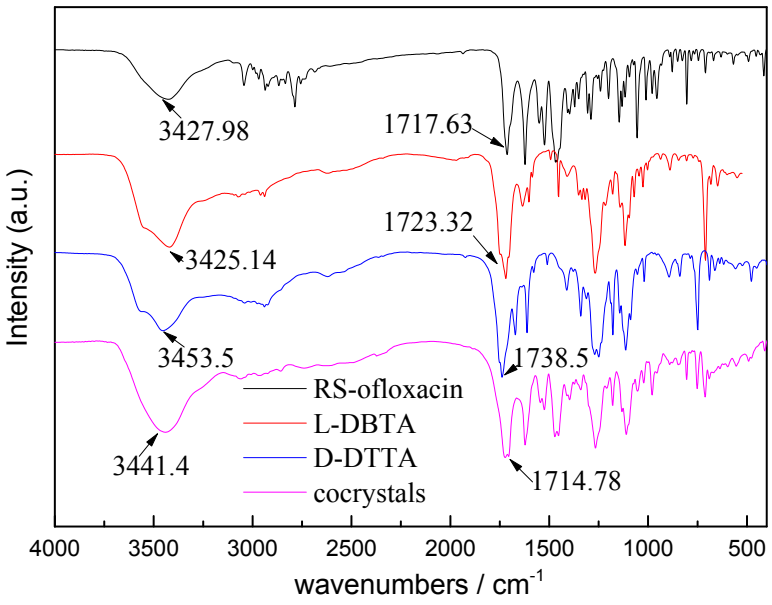

(b)

Figure. S2 FT-IR curves of the co-crystals obtained after the chiral selectivity transition process (a, D-DBTA and L-DTTA as chiral seletor, b, L-DBTA and D-DTTA as chiral selector)

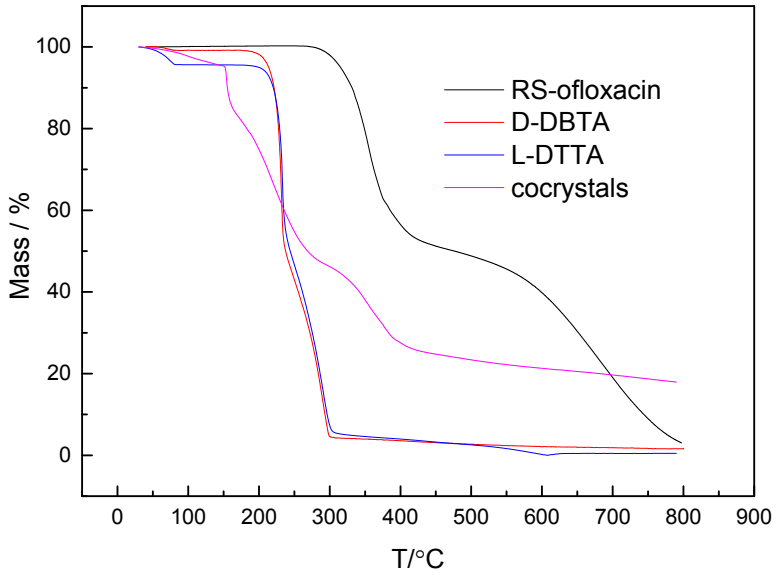

(a)

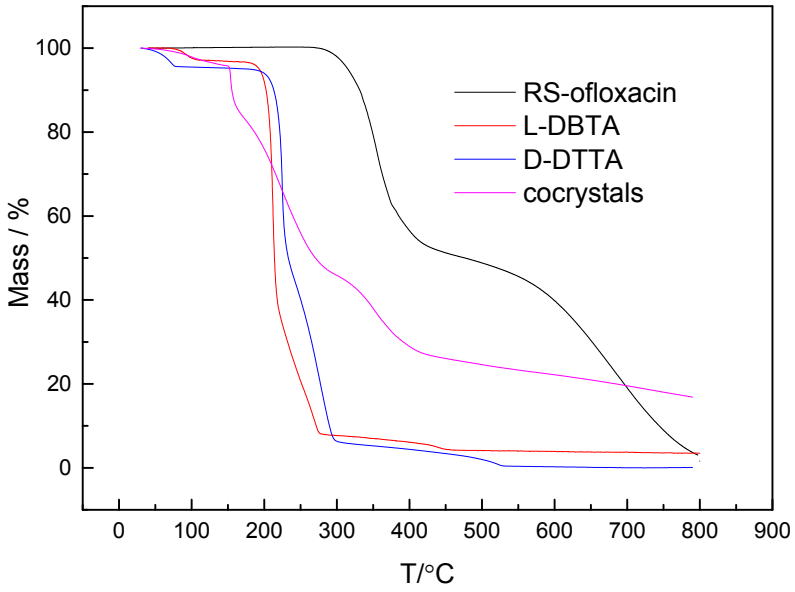

(b)

Figure. S3 TGA curves of the co-crystals obtained after the chiral selectivity transition process (a, D-DBTA and L-DTTA as chiral selector; b, L-DBTA and D-DTTA as chiral selector)

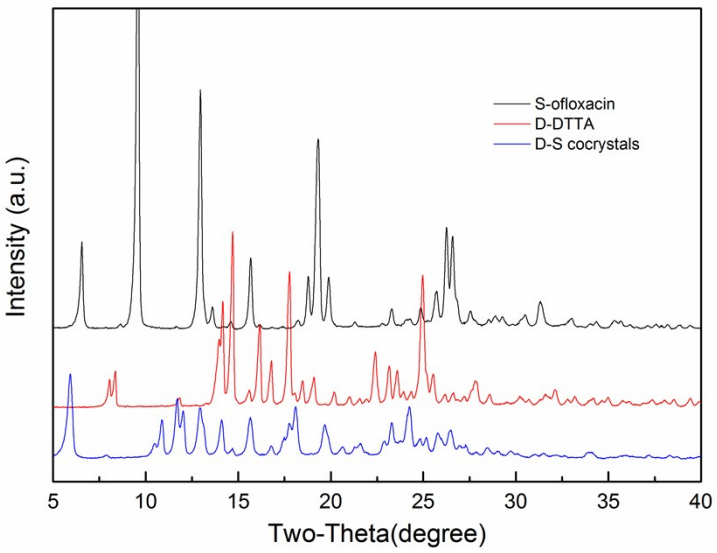

(a)

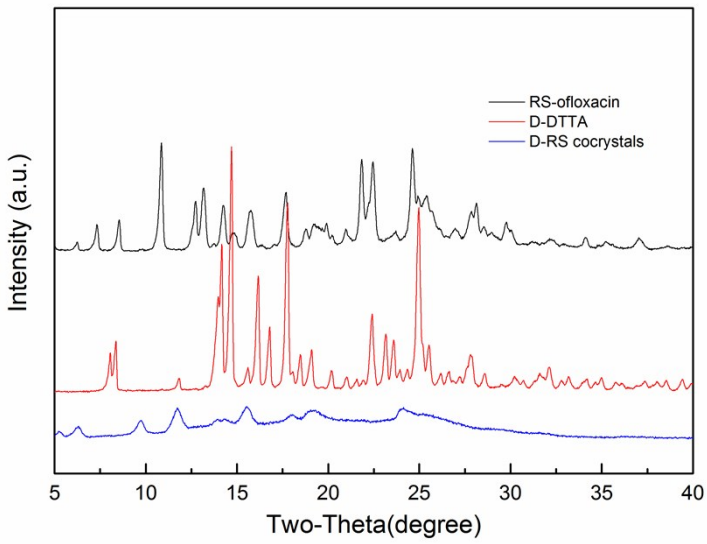

(b)

Figure. S4 PXRD spectra of the co-crystals prepared by slurry reaction experiments. (a, D-DTTA:S-OFLX, b, D-DTTA:RS-OFLX)

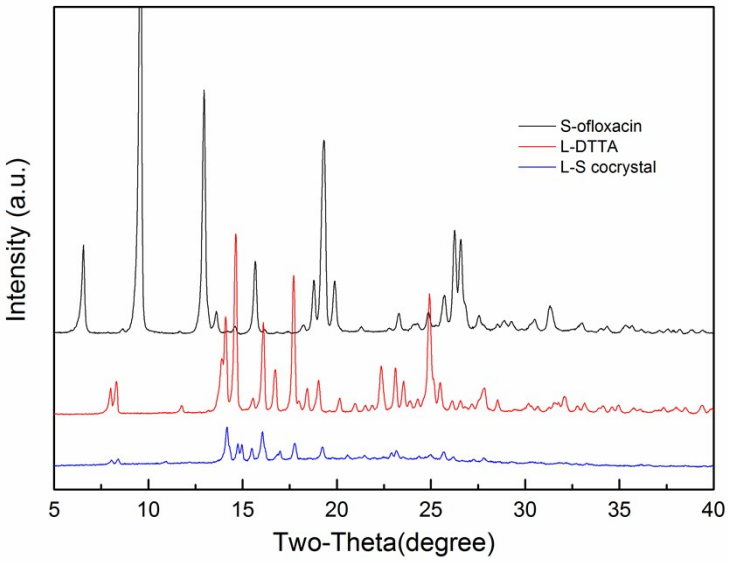

(a)

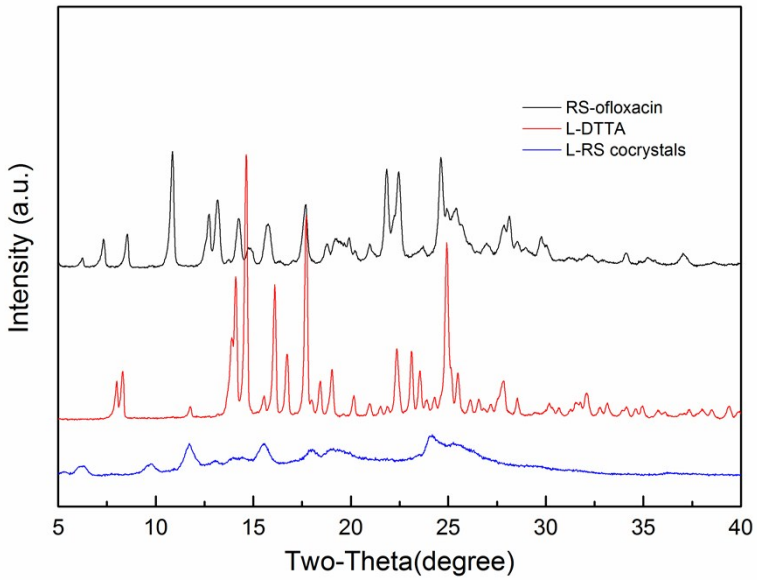

(b)

Figure. S5 PXRD spectra of the co-crystals prepared by slurry reaction experiments. (a, L-DTTA:S-OFLX, b, L-DTTA:RS-OFLX)

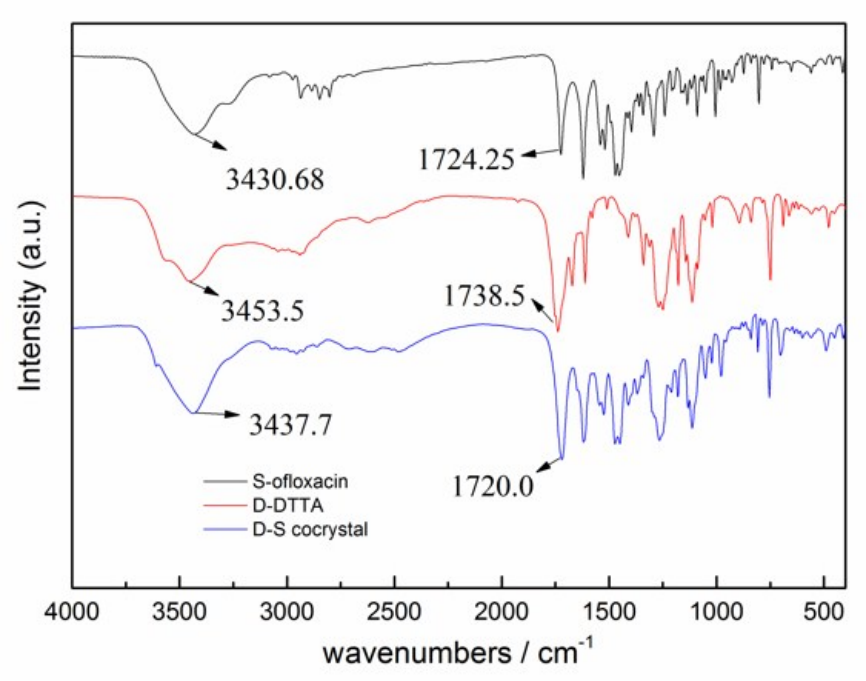

(a)

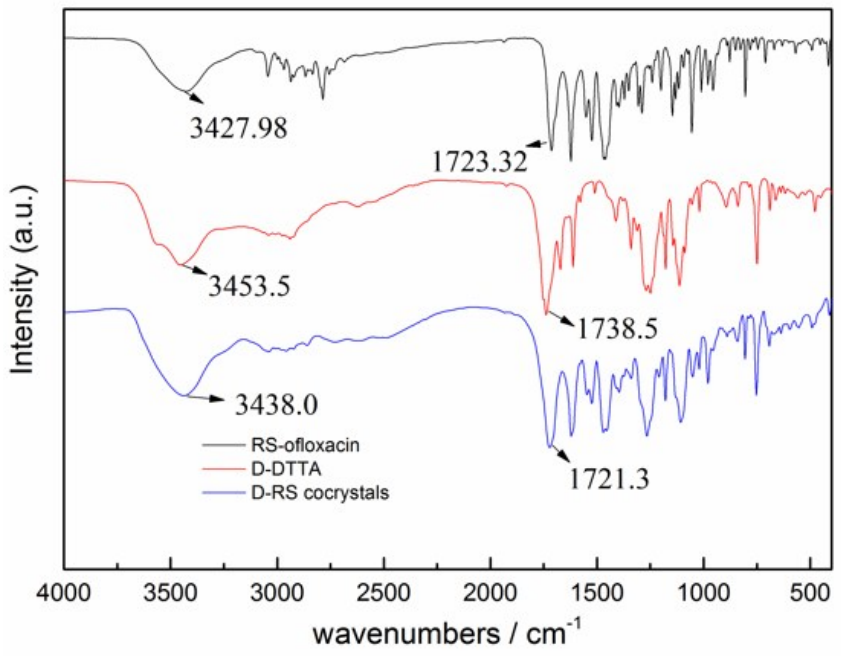

(b)

Figure. S6 FT-IR spectra of the co-crystals prepared by slurry reaction experiments. (a, D-DTTA:S-OFLX, b, D-DTTA:RS-OFLX)

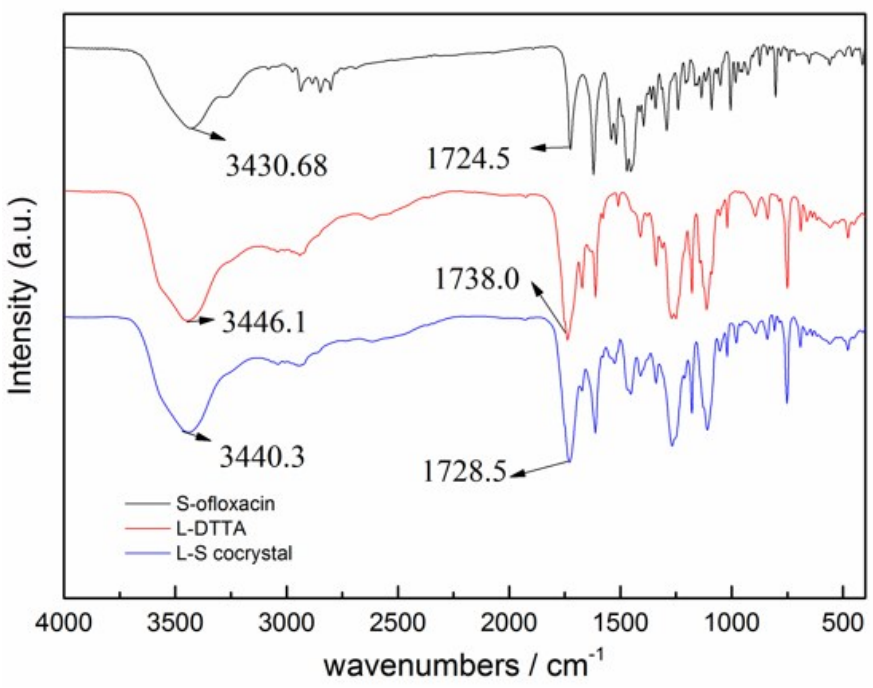

(a)

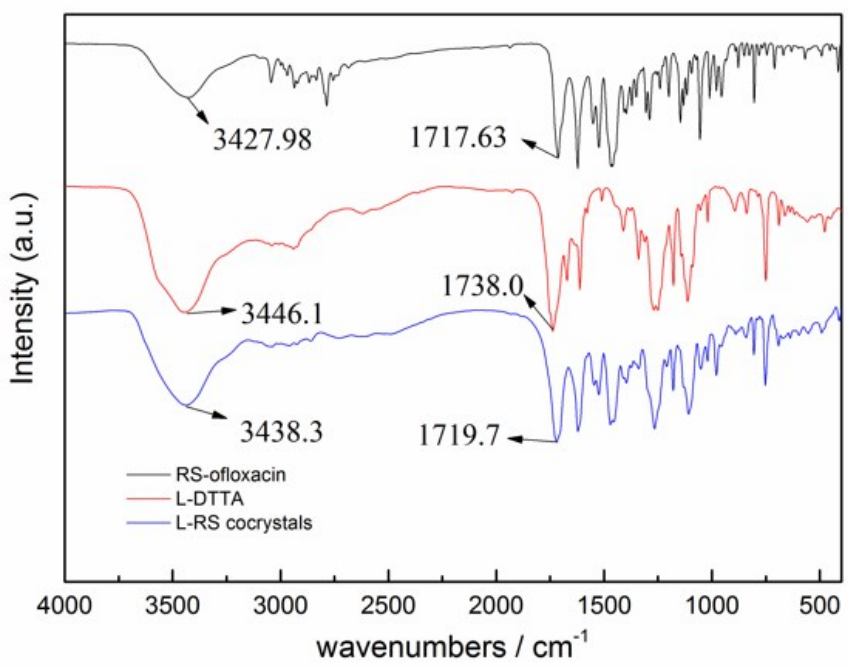

(b)

Figure. S7 FT-IR spectra of the co-crystals prepared by slurry reaction experiments. (a, L-DTTA:S-OFLX, b, L-DTTA:RS-OFLX)

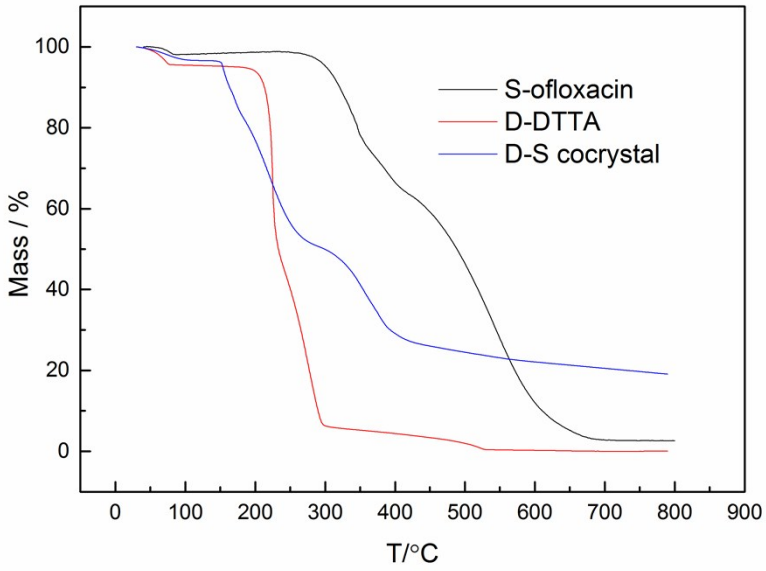

(a)

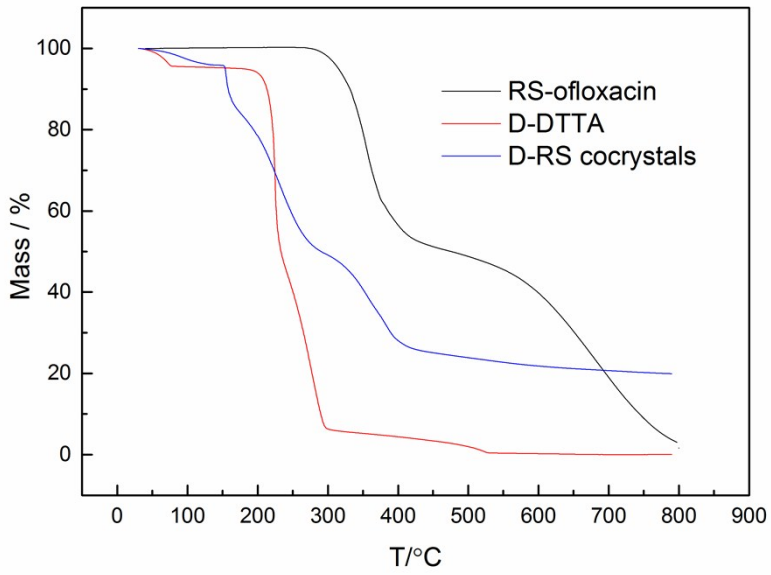

(b)

Figure. S8 TG spectra of the co-crystals prepared by slurry reaction experiments. (a, D-DTTA:S-OFLX, b, D-DTTA:RS-OFLX)

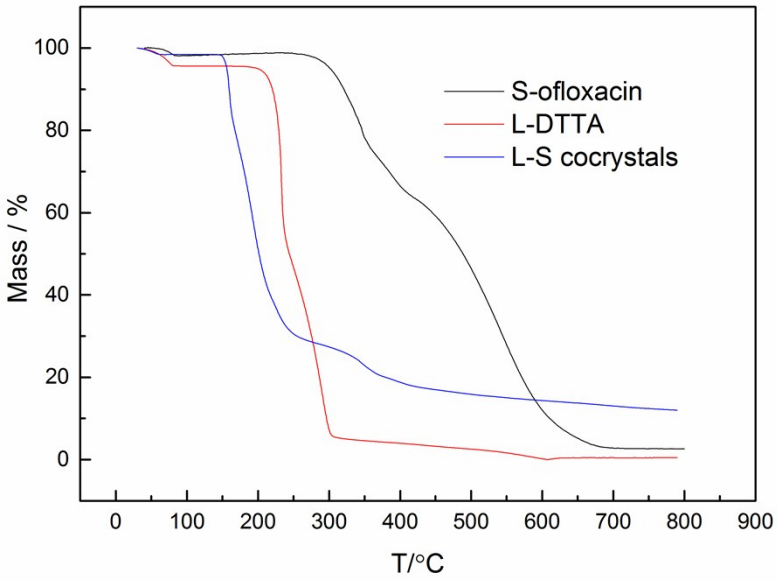

(a)

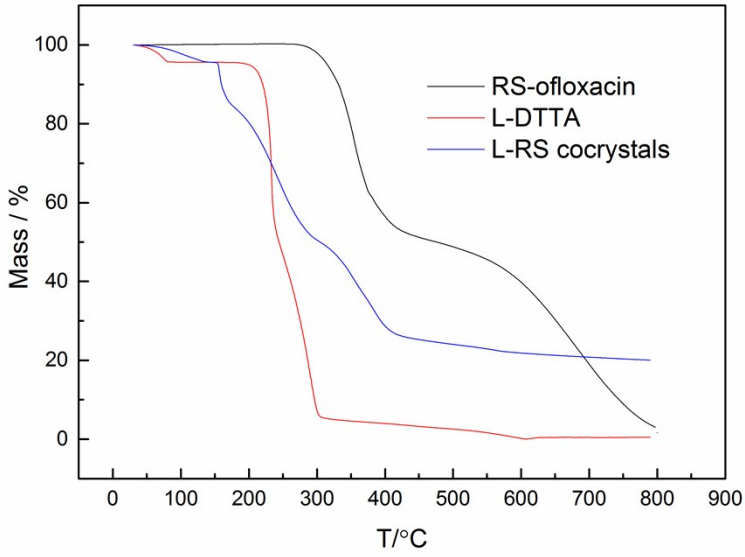

(b)

Figure. S9 TG spectra of the co-crystals prepared by slurry reaction experiments. (a, L-DTTA:S-OFLX, b, L-DTTA:RS-OFLX)